Research Article | Vol. 31, No. 22 / 23 Oct 2023 / Optics Express 36836
Optics EXPRESS

Order transfer in a hybrid Raman-laser-optomechanical resonator

ZHENNING YANG,[1] WANZHE ZHANG,[1,2,3] CHANGLONG ZHU,[1,4] ZHE WANG,[1] JIANQING GUAN,[1] YUE HUO,[1] XIAOHE TANG,[1] WEI SHI,[1] KEYU XIA,[5] YU-XI LIU,[6] LAN YANG,[7] AND JING ZHANG[8,9,*]

[1]*Department of Automation, Tsinghua University, Beijing 100084, China*
[2]*China Mobile Group Co., Ltd, Beijing 100084, China*
[3]*China Mobile Information System Integration Co., Ltd, Beijing 100084, China*
[4]*Max Planck Institute for the Science of Light, Staudtstr. 2, 91058 Erlangen, Germany*
[5]*College of Engineering and Applied Sciences, Nanjing University, Nanjing 210023, China*
[6]*Institute of Microelectronics, Tsinghua University, Beijing 100084, China*
[7]*Department of Electrical and Systems Engineering, Washington University, St. Louis, Missouri 63130, USA*
[8]*MOE Key Lab for Intelligent Networks and Network Security, Xi'an Jiaotong University, Xi'an 710049, China*
[9]*School of Automation Science and Engineering, Xi'an Jiaotong University, Xi'an 710049, China*
[*]*zhangjing2022@xjtu.edu.cn*

Abstract: Order is one of the most important concepts to interpret various phenomena such as the emergence of turbulence and the life-evolution process. The generation of laser can also be treated as an ordering process in which the interaction between the laser beam and the gain medium leads to the correlation between photons in the output optical field. Here, we demonstrate experimentally in a hybrid Raman-laser-optomechanical system that an ordered Raman laser can be generated from an entropy-absorption process by a chaotic optomechanical resonator. When the optomechanical resonator is chaotic or disordered enough, the Raman-laser field is in an ordered lasing mode. This can be interpreted by the entropy transfer from the Raman-laser mode to the chaotic motion mediated by optomechanics. Different order parameters, such as the box-counting dimension, the maximal Lyapunov exponent, and the Kolmogorov entropy, are introduced to quantitatively analyze this entropy transfer process, by which we can observe the order transfer between the Raman-laser mode and the optomechanical resonator. Our study presents a new mechanism of laser generation and opens up new dimensions of research such as the modulation of laser by optomechanics.

1. Introduction

Order is a quantity commonly describing particular states with randomness or uncertainty. Order exists in many systems and can be evaluated by entropy in the second law of thermodynamics. In the second law of thermodynamics, the change of the system's entropy is induced by the information flow between the system and its environment. In a broader case, the change of the degrees of order is induced by the exchange of matter and energy between the system and its environment. This exchange of matter and energy leads to the so-called generalized second law of thermodynamics [1]. According to the second law of thermodynamics, the entropy of any isolated system always increases, which means that the isolated system spontaneously changes from an ordered state to a disordered state [2]. However, the opposite process, i.e., the entropy-decreasing process or the so-called ordering process, is more interesting. It often leads to various meaningful phenomena, e.g., the evolution of life and species. The stationary states of the ordering processes are called dissipative structures. To realize a dissipative structure, the system should be open,

#502262 https://doi.org/10.1364/OE.502262
Journal © 2023 Received 4 Aug 2023; revised 17 Sep 2023; accepted 18 Sep 2023; published 17 Oct 2023

Optics EXPRESS

i.e., to exchange entropy, matter, or energy with the outside world continuously, and far away from the equilibrium state. When changes in the external conditions achieve certain threshold values, the stable and ordered dissipative structures can be spontaneously generated by the role of the internal self-organization phenomena [3]. These ordering processes and the generation of dissipative structures can be seen in many systems, such as quantum systems [4–6] and biological systems [7,8]. In addition, many new ordered structures can be realized in different materials such as metals [9,10], antiferromagnets [11], glasses [12,13], and polymers [14,15].

A laser can also be generated by an ordering process [16–21]. When the photon with a fixed frequency outcompete the action of other photons, it is strengthened and occupies a dominant position. The process of ordering in the laser is completed when the pump power achieves a threshold value and the individual photons behave in a fully correlated manner. The ordered states of lasers can also be treated as dissipative structures [22]. As a special kind of laser, the Raman laser is realized by scattering processes caused by the vibrations of molecules, and it can be widely used in various aspects such as creating a cascaded laser source [23]. With the development of related technologies, nonlinear Raman source in optical microresonators and enhanced Raman scattering has been presented [24,25]. Raman lasers have also been successfully demonstrated in on-chip microresonators under on-demand control [26] and used for ordering process demonstration [27] recently.

Optomechanics is another important phenomenon that can be achieved in microresonators [28]. It has been used for quantum information processing [29], detection of gravitational waves [30,31], and optical-to-microwave conversion [32]. Disordered chaotic vibrations can also be excited in optomechanical resonators with increasing optical input powers [33–36]. However, the ordered laser effects and disordered chaotic motions are somewhat conflicted so that they are hardly observed simultaneously.

In this work, we report the experiments that ordered Raman laser and disordered chaos can be shown simultaneously in a hybrid Raman-laser-optomechanical system. In this hybrid system, four modes are involved: an optical pump mode in the 1550 nm band, an optical Raman-laser mode in the 1676 nm band, a mechanical mode, and a molecular vibration mode. It has been demonstrated that the Raman laser is enhanced in this hybrid system when the optomechanical resonator turns to be more chaotic and disordered. This can be explained by the entropy-decreasing at the Raman-laser degree absorbed by an external disordered source, making the Raman-laser degree more ordered and finally stabilized at a localized state. Different order parameters such as the box-counting dimension, the maximal Lyapunov exponent, and the Kolmogorov entropy are introduced to quantitatively analyze this entropy-transfer process. Furthermore, the phase transition and the bifurcation diagram of the hybrid system during the formation of the dissipative structures are also analyzed.

2. Characterization of the hybrid Raman-laser-optomechanical resonator

The schematic diagram of our hybrid Raman-laser-optomechanical resonator is shown in Fig. 1(a). A tunable pump laser in the 1550 nm wavelength band is used to generate a Raman laser in a silica microtoroid with the major diameter of about 50 μm. A fiber taper is used to couple the pump light into the microtoroid resonator. When the mechanical motion of the microtoroidal optomechanical resonator transits from the periodic regime to the chaotic regime, the vibrations of silica molecules are excited, resulting in the generation of an ordered Raman laser.

The system we consider here is a hybrid Raman-laser-optomechanical resonator, which is composed of four modes: an optical pump mode with complex amplitude a_p, a Raman-laser mode with complex amplitude a_R and eigenfrequency ω_c, the mechanical mode with complex amplitude b_m and frequency Ω_m, and the molecular vibration mode with complex amplitude b_v and frequency Ω_v [Fig. 1(b)]. The optical cavity modes are coupled to the mechanical mode via the radiation forces, which can be seen as an equivalent Fabry-Perot cavity with one moving

Optics EXPRESS

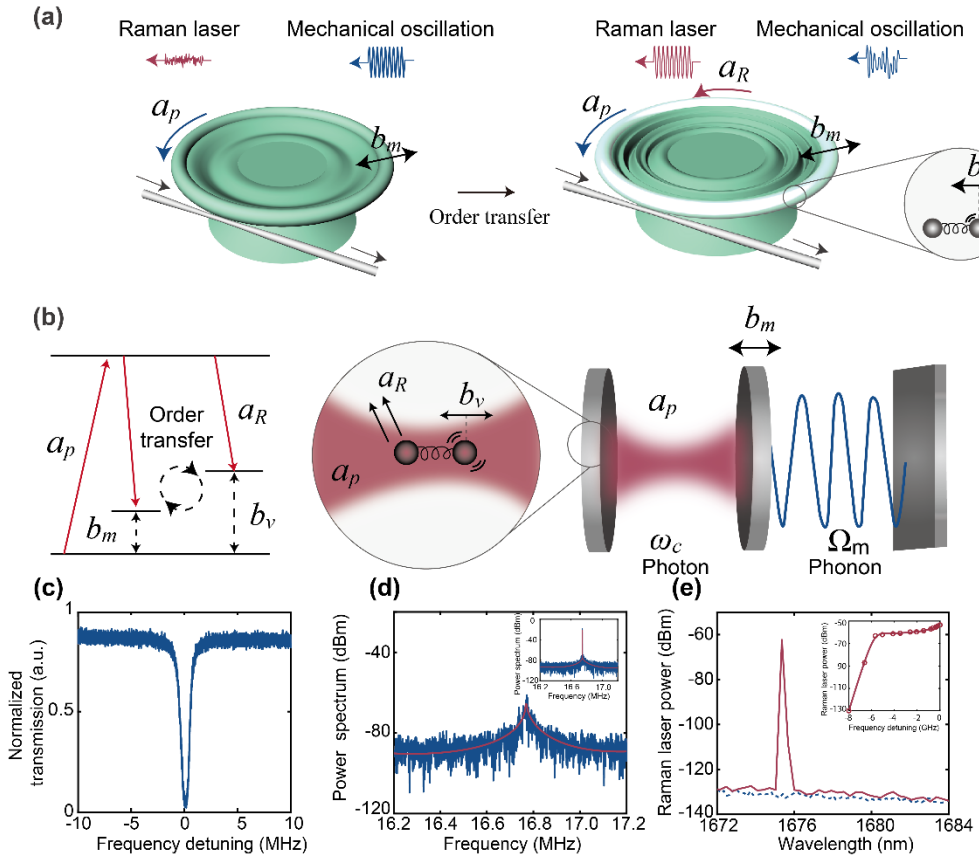

Fig. 1. The hybrid Raman-laser-optomechanical resonator. (a) Cross section of the Raman-laser-optomechanical microtoroid resonator showing the indirect interaction mediated by the optical pump mode between the mechanical motion of the microtoroid resonator and the Raman-laser mode. (b) Schematic diagram of the indirect coupling between the Raman-laser mode and the mechanical vibration of the cavity mediated by the optical pump mode in a Fabry-Perot cavity with one moving end mirror. (c) The normalized transmission of the optical pump mode in the 1550 nm band with a quality factor of 4.2×10^7. (d) The mechanical mode with a quality factor of 1.2×10^3 below the threshold of the mechanical instability. Inset shows the spectrum above the threshold of the mechanical instability with increasing pump power. Blue curves, experimental data; red curves, best fitting curves. (e) The spectrum of the Raman-laser mode in the 1676 nm band is read by the optical spectrum analyzer (OSA). The Raman-laser mode is below the threshold (blue curve) and excited (red curve) with increasing pump power. The inset shows the threshold curve of the Raman-laser mode.

Optics EXPRESS

mirror. The motion of the mirror changes the length of the cavity and thus induces an effective frequency shift to the optical cavity mode. The shift leads to effective optomechanical couplings with strength G_m. The coupling between the cavity modes and the molecular vibration mode can also be modeled as an optomechanical-type coupling, resulting in the formation of the Raman laser mode through their interaction. In such a model, the molecular mode interacts with the cavity modes just like a plasmonic cavity mode interacts with the optical mode.

As shown in Fig. 1(c), the quality factor of the optical mode is 4.2×10^7. The mechanical mode shown in Fig. 1(d) has a central frequency of 16.7 MHz and a mechanical quality factor of 1.2×10^3 when the pump power is below the threshold of the mechanical instability, and the linewidth of the mechanical mode will be narrowed when the pump power is above the threshold. (see Fig. 1(d), inset). The frequency spectrum of the Raman-laser mode is shown in Fig. 1(e). The (blue) red curve represents the case that the Raman laser is (not) excited. Figure 1(e) shows the resonance peak of the Raman-laser mode at about 1676 nm. The inset of Fig. 1(e) displays the threshold curve of the Raman-laser mode.

3. Order transfer from the optomechanical resonator to the Raman-laser mode

When varying particular system parameters, we can see the energy and order transfers between different components of the hybrid Raman-laser-optomechanical resonator. Figure 2(a) shows the time-domain signals of the optomechanical output field of the microtoroid resonator (upper blue curve) and the Raman-laser mode (lower red curve), respectively. By changing the frequency detuning between the input pump field and the cavity mode in the 1550 nm band, we obtain two different regimes in the blue-detuned regime. As the frequency detuning ranges from -4.3 GHz to -9.3 GHz (pink regime in Fig. 2(a)), the optomechanical motion of the resonator is periodic. Thus, this regime is referred to as the ordered mechanical regime. However, the Raman-laser mode is below the threshold, and the time-domain Raman-laser signal is disordered in this regime. When the frequency detuning exceeds -4.3 GHz (yellow regime in Fig. 2(a)), the phase transition takes place and new dissipative structures are gradually generated, under which the optomechanical mode is totally chaotic (disordered), and the Raman-laser mode is far above the threshold and thus generates an ordered output lasing field.

The phase transition process can be seen more clearly in the phase diagrams in Fig. 2(b-e), and the insets are the corresponding time-domain signals. In the ordered mechanical regime, when the frequency detuning is assigned as -6.8 GHz, as shown in Figs. 2(b, c), the phase diagram of the optomechanical mode is a single limit cycle and the Raman-laser mode is in a mess. This is confirmed by the sinusoidal time-domain signal of the optomechanical mode and the noisy time-domain signal for the Raman-laser mode, as shown in the insets of Fig. 2(b, c). When the frequency detuning is changed to -0.3 GHz, the system enters the ordered Raman-laser regime, while the optomechanical mode is totally chaotic (disordered), see Fig. 2(d). In contrast, the Raman-laser mode shown in Fig. 2(e) follows a single limit cycle and thus is periodic. In this regime, the order has been transferred from the optomechanical mode to the Raman-laser mode.

To give more insights for the above-illustrated phase transition process, we introduce different order parameters to quantitively analyze the order transfer from the optomechanical resonator to the Raman-laser mode. Among all the order parameters, the box-counting dimension, the maximal Lyapunov exponent, and the Kolmogorov entropy are the most intuitive indicators in order transfer analysis. They also each have a rigorous criterion for determining whether a system is disordered. For example, integer and fractional values of the system's box-counting dimension correspond to ordered and disordered states, respectively. System order can also be determined by assessing whether the Kolmogorov entropy and the maximum Lyapunov exponent are greater than 0.

Let us first check the box-counting dimension of different system components, as shown in Fig. 3(a) (see the definition of the box-counting dimension in Supplement 1). The box-counting

Optics EXPRESS

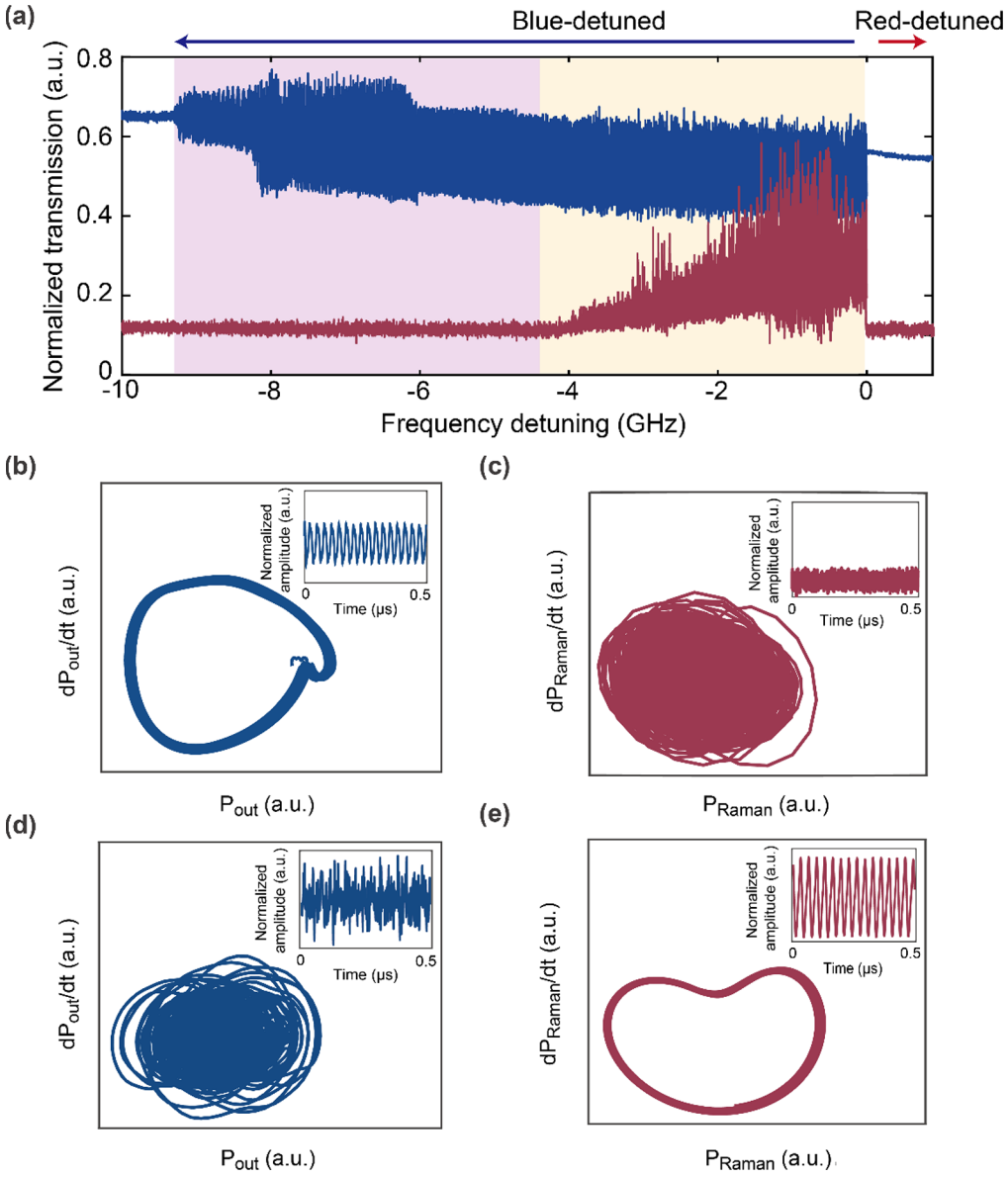

Fig. 2. Time evolution of the hybrid Raman-laser-optomechanical resonator. (a) Different regimes are obtained by varying the frequency detuning between the pump mode and the cavity mode. The optomechanical mode (upper blue curve) and the Raman-laser mode (lower red curve) show two different regimes: the ordered mechanical regime (pink regime), and the ordered Raman laser regime (yellow regime). The phase diagrams are plotted by the derivatives of the output powers of the optomechanical mode and the Raman-laser mode versus the respective output powers. The phase diagrams of the optomechanical mode are presented in the ordered mechanical regime (b), the ordered Raman laser regime (d), and the corresponding phase diagrams of the Raman-laser mode are shown in (c) and (e).

Optics EXPRESS

dimension is a method used to quantify the spatial filling of a fractal set through the system phase diagram. Its fundamental concept involves evaluating how the count of boxes needed changes as the box size is adjusted. The box-counting dimension of an ordered structure is always an integer, while the disordered dissipative structure such as a chaotic attractor always has a fractal box-counting dimension. The box-counting dimension of the dissipative structure will increase when it turns to be more chaotic. In fact, we use the time series obtained in the experiment for calculation, so the time series are not perfectly periodic signals. The time series contains noise, so the box-counting dimension of the optomechanical mode is larger than 1 although the dynamics is a limit cycle. In Fig. 3(a), two different regimes are achieved by changing the frequency detuning. The box-counting dimension of the Raman-laser mode (red dashed curve) decreases and that of the optomechanical mode (blue solid curve) increases in the ordered mechanical regime. It means that order is gradually transferred from the optomechanical mode to the Raman-laser mode. When the frequency detuning is above the threshold of the Raman laser, that is in the ordered Raman laser regime, the box-counting dimension of the Raman-laser mode decreases rapidly and that of the optomechanical mode increases fast and stably. This means that the phase transition occurs and the periodic (ordered) limit cycle of the Raman-laser mode and the chaotic (disordered) attractor of the optomechanical mode are constructed. During this process, the chaotic optomechanical oscillation absorbs entropy from the Raman-laser mode by which the ordered Raman laser is generated.

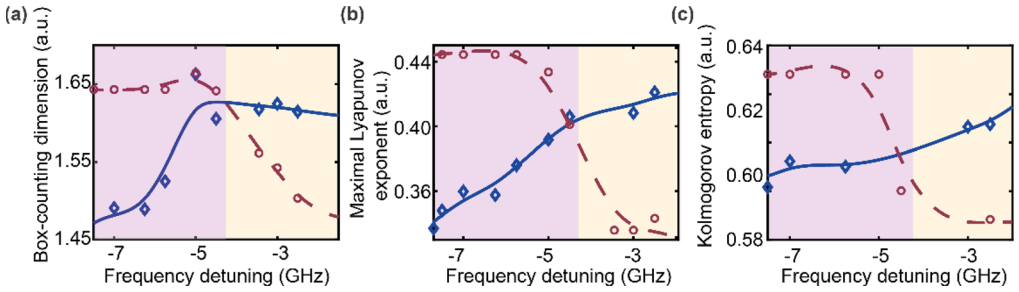

Fig. 3. Order transfer from the optomechanical mode to the Raman-laser mode is illustrated by different order parameters. (a) The box-counting dimension of the optomechanical mode (blue solid curve) and the Raman-laser mode (red dashed curve) versus the frequency detunings. (b) The maximal Lyapunov exponent of the optomechanical mode (blue solid curve) and the Raman-laser mode (red dashed curve) versus the frequency detunings. (c) The K entropies of the optomechanical mode (blue solid curve) and the Raman-laser mode (red dashed curve) versus the frequency detunings.

Another metric for characterizing the order of the system is the maximal Lyapunov exponent (MLE), which quantizes the derivation between different phase trajectories. The MLE is negative in an ordered system, while in a chaotic system, the MLE is positive. The more chaotic the system is, the larger MLE will become. The trajectories of MLE under different frequency detunings of the optomechanical mode (blue solid curve) and the Raman-laser mode (red dash curve) are shown in Fig. 3(b). Due to the measurement noise, the MLE is positive when the stationary trajectory of the system is a limit cycle. As the frequency detuning increases in the ordered mechanical regime, the optomechanical mode will gradually evolve from the periodic regime to the chaotic regime, while the signals of the Raman-laser mode become more orderly. Finally, the Raman-laser mode is sinusoidal and the hybrid system enters the ordered Raman-laser regime. In the ordered Raman-laser regime, the MLE of the optomechanical mode will remain higher than that of the Raman-laser mode.

The third parameter we introduce is the Kolmogorov entropy, which is also called K entropy in short. K entropy is a kind of entropy introduced to describe the degree of confusion (see the

Optics EXPRESS

definition of the K entropy in Supplement 1). It quantifies the rate at which trajectories diverge, indicating how quickly new information emerges as the system undergoes evolution. In the chaotic system, the K entropy is greater than 0. The larger the K entropy is, the more chaotic the system is. To characterize the two regimes, we tune the frequency detuning and check the K entropy of the hybrid Raman-laser-optomechanical resonator in Fig. 3(c). The time series contains noise, so the K entropy is larger than 0 although the system trajectory is a limit cycle. In the ordered mechanical regime, the K entropy of the optomechanical mode (blue solid curve) increases while that of the Raman-laser mode (red dashed curve) decreases, and the two curves intersect with each other on the boundary of the ordered mechanical regime. In the ordered Raman laser regime, the changes of the K entropy also show that a stable periodic limit cycle and chaotic attractor are constructed for the Raman-laser mode and the optomechanical mode respectively.

To better understand the formation process of the new dissipative structures, we further introduce the signal-to-noise ratio (SNR) to evaluate the degree of order of the system. In the experiment, whenever we change a frequency detuning, we can obtain the corresponding SNRs of the Raman-laser mode from the optical spectrum analyzer (OSA) and optomechanical mode from the electrical spectrum analyzer (ESA) respectively (see the experimental setup in Supplement 1). With the increase of the SNR, the system turns to be more ordered. In Fig. 4(a), in the ordered mechanical regime, with the increase of the SNR (order) of the Raman-laser mode, the amplitude of the optomechanical mode increases without bifurcation, which means that the phase transition does not occur in this case. In the ordered Raman laser regime, with the increase of the SNR of the Raman-laser mode, the optomechanical mode will begin to bifurcate, and finally, a stable chaotic attractor is generated.

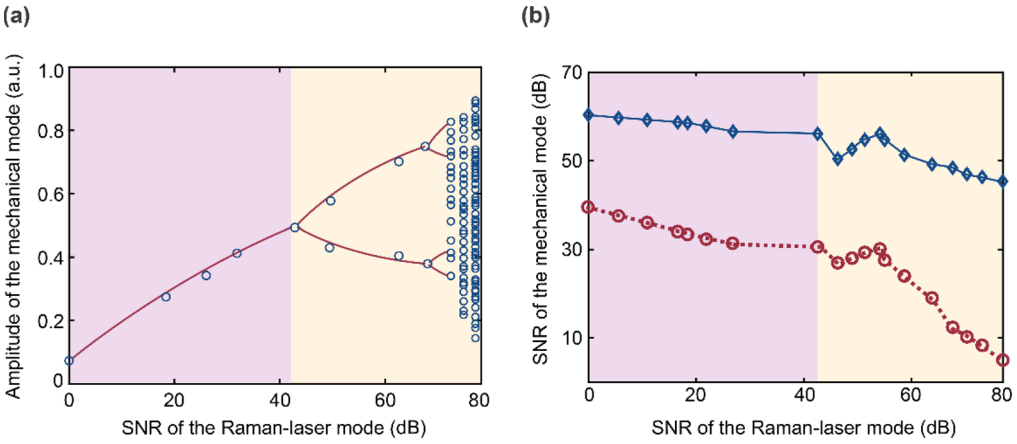

Fig. 4. Order transfer between the optomechanical mode and the Raman-laser mode in two different regimes. (a) The bifurcation diagram of the optomechanical mode versus the SNR (order) of the Raman-laser mode. Period-doubling bifurcation occurs for the optomechanical mode with the increase of the SNR of the Raman-laser mode. (b) The SNR of the optomechanical mode at the main peak (blue solid curve) and the period-doubling peak (red dashed curve) versus the SNR of the Raman-laser mode in the ordered mechanical regime, and the ordered Raman laser regime respectively.

In Fig. 4(b), the SNR of the optomechanical mode at the main peak (blue solid curve) and the period-doubling peak (red dashed curve) changes with the increase of the SNR of the Raman-laser mode. In the ordered mechanical regime, the SNR of the optomechanical mode decreases gradually with the increase of the SNR of the Raman-laser mode, which means that order is gradually transferred before the phase transition occurs. In the ordered Raman laser regime, the

Optics EXPRESS

SNR of the optomechanical mode stably decreases further with the increase of the SNR of the Raman-laser mode, which means that the order is transferred from the Raman-laser mode to the optomechanical mode further and new dissipative structures are generated. Additionally, we can see from Fig. 4(b) that the SNR of the optomechanical mode at the period-doubling peak (red dashed curve) changes more drastically than that at the main peak (blue solid curve), which means that the SNR of the optomechanical mode at the period-doubling peak is more sensitive and thus a more powerful tool to describe the order transfer between the two modes in the two different regimes.

4. Conclusion

In conclusion, we experimentally demonstrated that an ordered Raman laser can be generated via the entropy absorption of a disordered chaotic source. We introduced the box-counting dimension, the Kolmogorov entropy, and the SNR of different components, to quantitively analyze the order transfer from the optomechanical mode to the Raman-laser mode in the hybrid Raman-laser-optomechanical resonator. It was found that, in this ordered optomechanical system, the phase transition occurred and new dissipative structures were constructed during the order transfer process. The period-doubling bifurcation process of the optomechanical mode was experimentally observed. The steeper curve of the SNR of the period-doubling peak means better sensitivity for evaluating order transfer. Our work showed a new mechanism for realizing and controlling on-chip micro-lasers.

Funding. Leading Scholar of Xi'an Jiaotong University; Program for Innovative Talents and Teams in Jiangsu (JSSCTD202138); Army Research Office (W911NF1210026, W911NF1710189); National Key Research and Development Program of China (2017YFA0303703, 2019YFA0308700); Wenhai Program of the S&T Fund of Shandong Province for Pilot National Laboratory for Marine Science and Technology (LSKJ202200900); National Science Foundation (EFMA1641109); Guoqiang Institute, Tsinghua University (20212000704); Joint Fund of Science & Technology Department of Liaoning Province and State Key Laboratory of Robotics (2021-KF-22-01); Innovative leading talent project of "Shuangqian plan" in Jiangxi Province; National Defense Basic Scientific Research Program of China (JCKY2019407C002); Tsinghua-Foshan Innovation Special Fund (TFISF); National Natural Science Foundation of China (11674194, 11874212, 11890704, 12004044).

Disclosures. The authors declare no conflicts of interest.

Data availability. Data underlying the results presented in this paper are not publicly available at this time but may be obtained from the authors upon reasonable request.

Supplemental document. See Supplement 1 for supporting content.

References

1. M. Kaviany, *Principles of Heat Transfer in Porous Media* (Springer Science & Business Media, 2012).
2. K. Manjunath and S. C. Kaushik, "Second law thermodynamic study of heat exchangers: A review," Renewable Sustainable Energy Rev. **40**, 348–374 (2014).
3. G. Nicolis and I. Prigogine, *Self-Organization in Nonequilibrium Systems: From Dissipative Structures to Order through Fluctuations* (Wiley, 1977).
4. J. S. Bernier, M. J. Lawler, and Y. B. Kim, "Quantum order by disorder in frustrated diamond lattice antiferromagnets," Phys. Rev. Lett. **101**(4), 047201 (2008).
5. L. P. Henry and T. Roscilde, "Order-by-disorder and quantum coulomb phase in quantum square ice," Phys. Rev. Lett. **113**(2), 027204 (2014).
6. J. R. Wootton and J. K. Pachos, "Bringing order through disorder: localization of errors in topological quantum memories," Phys. Rev. Lett. **107**(3), 030503 (2011).
7. J. Buhl, D. J. Sumpter, I. D. Couzin, J. J. Hale, E. Despland, E. R. Miller, and S. J. Simpson, "From disorder to order in marching locusts," Science **312**(5778), 1402–1406 (2006).
8. H.E.A. Macgregor, J. E. Herbert-Read, and C. C. Ioannou, "Information can explain the dynamics of group order in animal collective behaviour," Nat. Commun. **11**(1), 1–8 (2020).
9. D.-A. Luh, C.-M. Cheng, C.-T. Tsai, K.-D. Tsuei, and J.-M. Tang, "Transition from disorder to order in thin metallic films studied with angle-resolved photoelectron spectroscopy," Phys. Rev. Lett. **100**(2), 027603 (2008).
10. Y. Motome, N. Furukawa, and N. Nagaosa, "Competing orders and disorder-induced insulator to metal transition in manganites," Phys. Rev. Lett. **91**(16), 167204 (2003).
11. P. Guruciaga, M. Tarzia, M. Ferreyra, L. Cugliandolo, S. Grigera, and R. Borzi, "Field-tuned order by disorder in frustrated ising magnets with antiferromagnetic interactions," Phys. Rev. Lett. **117**(16), 167203 (2016).

Optics EXPRESS

12. L. O. Hedges, R. L. Jack, J. P. Garrahan, and D. Chandler, "Dynamic order-disorder in atomistic models of structural glass formers," Science **323**(5919), 1309–1313 (2009).
13. P. Yunker, Z. Zhang, and A. G. Yodh, "Observation of the disorder-induced crystal-to-glass transition," Phys. Rev. Lett. **104**(1), 015701 (2010).
14. T. Hashimoto, N. Amino, S. Nishitsuji, and M. Takenaka, "Hierarchically self-organized filler particles in polymers: cascade evolution of dissipative structures to ordered structures," Polym. J. **51**(2), 109–130 (2019).
15. G. A. Mcconnell, A. P. Gast, J. S. Huang, and S. D. Smith, "Disorder-order transitions in soft sphere polymer micelles," Phys. Rev. Lett. **71**(13), 2102–2105 (1993).
16. H. Haken, *Synergetics: A Workshop Proceedings of the International Workshop on Synergetics at Schloss Elmau, Bavaria* (Springer Science & Business Media, 1977).
17. L. Yang, T. Carmon, B. Min, S. M. Spillane, and K. J. Vahala, "Erbium-doped and Raman microlasers on a silicon chip fabricated by the sol-gel process," Appl. Phys. Lett. **86**(9), 091114 (2005).
18. B. Peng, S. K. Özdemir, S. Rotter, H. Yilmaz, M. Liertzer, F. Monifi, C. M. Bender, F. Nori, and L. Yang, "Loss induced suppression and revival of lasing," Science **346**(6207), 328–332 (2014).
19. J. Zhang, B. Peng, S. K. Özdemir, K. Pichler, D. O. Krimer, G. Zhao, F. Nori, Y. Liu, S. Rotter, and L. Yang, "A phonon laser operating at an exceptional point," Nat. Photonics **12**(8), 479–484 (2018).
20. Ren-Min. Ma, "Lasing under ultralow pumping," Nat. Mater. **18**(11), 1152–1153 (2019).
21. Y. Kong, F. Bo, W. Wang, D. Zheng, H. Liu, G. Zhang, R. Rupp, and J. Xu, "Recent progress in lithium niobate: optical damage, defect simulation, and on-chip devices," Adv. Mater. **32**(3), 1806452 (2020).
22. H. Haken, *Advanced Synergetics: Instability Hierarchies of Self-Organizing Systems and Devices* (Springer, 1983).
23. H. Rong, S. Xu, O. Cohen, O. Raday, M. Lee, V. Sih, and M. Paniccia, "A cascaded silicon Raman laser," Nat. Photonics **2**(3), 170–174 (2008).
24. S. M. Spillane, T. J. Kippenberg, and K. J. Vahala, "Ultralow-threshold Raman laser using a spherical dielectric microcavity," Nature **415**(6872), 621–623 (2002).
25. G. Zhao, S. K. Ozdemir, T. Wang, L. Xu, G.-L. Long, and L. Yang, "Raman lasing and Fano lineshapes in a packaged fiber-coupled whispering-gallerymode microresonator," Sci. Bull. **62**(12), 875–878 (2017).
26. X. Yang, S. K. Özdemir, B. Peng, H. Yilmaz, F. C. Lei, G. L. Long, and L. Yang, "Raman gain induced mode evolution and on-demand coupling control in whispering-gallery-mode microcavities," Opt. Express **23**(23), 29573–29583 (2015).
27. B. H. Hokr, J. N. Bixler, M. T. Cone, J. D. Mason, H. T. Beier, G. D. Noojin, G. I. Petrov, L. A. Golovan, R. J. Thomas, and B. A. Rockwell, "Bright emission from a random Raman laser," Nat. Commun. **5**(1), 1–5 (2014).
28. M. Aspelmeyer, T. J. Kippenberg, and F. Marquardt, "Cavity optomechanics," Rev. Mod. Phys. **86**(4), 1391–1452 (2014).
29. K. Stannigel, P. Rabl, A. S. Sørensen, M. D. Lukin, and P. Zoller, "Optomechanical transducers for quantum-information processing," Phys. Rev. A **84**(4), 042341 (2011).
30. A. Abramovici, W. E. Althouse, R. Drever, Y. Gursel, S. Kawamura, F. J. Raab, D. Shoemaker, L. Sievers, R. E. Spero, and K. S. Thorne, "LIGO: The laser interferometer gravitational-wave observatory," Science **256**(5055), 325–333 (1992).
31. LIGO Scientific Collaboration and Virgo Collaboration, "Observation of gravitational waves from a binary black hole merger," Phys. Rev. Lett. **116**(6), 061102 (2016).
32. L. Shao, M. Yu, S. Maity, N. Sinclair, and M. Lončar, "Microwave-to-optical conversion using lithium niobate thin-film acoustic resonators," Optica **6**(12), 1498–1505 (2019).
33. L. Bakemeier, A. Alvermann, and H. Fehske, "Route to chaos in optomechanics," Phys. Rev. Lett. **114**(1), 013601 (2014).
34. T. Carmon, M. C. Cross, and K. J. Vahala, "Chaotic quivering of micron-scaled on-chip resonators excited by centrifugal optical pressure," Phys. Rev. Lett. **98**(16), 167203 (2007).
35. F. Monifi, J. Zhang, S. K. Özdemir, B. Peng, Y. X. Liu, F. Bo, F. Nori, and L. Yang, "Optomechanically induced stochastic resonance and chaos transfer between optical fields," Nat. Photonics **10**(6), 399–405 (2016).
36. Y.-J. Qian, Q.-T. Cao, S. Wan, Y.-Z. Gu, L.-K. Chen, C.-H. Dong, Q. Song, Q. Gong, and Y.-F. Xiao, "Observation of a manifold in the chaotic phase space of an asymmetric optical microcavity," Photonics Res. **9**(3), 364–369 (2021).